Electronic Supplementary Material (ESI) for Journal of Materials Chemistry A.
This journal is © The Royal Society of Chemistry 2017

Supporting Information

Stable Hierarchical Microspheres of 1D Fe-Gallic Acid MOFs for Fast and Efficient Cr (VI) Elimination by a Combination of Reduction, Metal Substitution and Coprecipitation

Hongyun Niu[a], Yang Zheng[a,b], Saihua Wang[a,b], Sijing He[a,b], Yaqi Cai[a,b,c]*

[a] State Key Laboratory of Environmental Chemistry and Ecotoxicology, Research Center for Eco-Environmental Sciences, Chinese Academy of Sciences, Beijing 100085, China.
[b] University of Chinese Academy of Sciences, Beijing, 100049, China.
[c] Institute of Environment and Health, Jianghan University, Wuhan 430056, China

E-mail: caiyaqi@rcees.ac.cn;
Tel: +86-10-6284-9182

Chemicals and Materials. All reagents were of analytical reagent grade and used without further purification. $FeCl_2 \cdot 4H_2O$, $FeCl_3 \cdot 6H_2O$, $K_2Cr_2O_7$, $CrCl_3$, $Zn(NO_3)_2 \cdot 6H_2O$, $MnCl_2 \cdot 4H_2O$, $BaCl_2 \cdot 2H_2O$, $Cu(NO_3)_2 \cdot 3H_2O$, $CrCl_3$, $CdCl_3 \cdot 6H_2O$, gallic acid, ethanol, and N,N-dimethylformamide (DMF, 99.5%) were purchased from Sinopharm Chemistry Reagent Co., Ltd. (Beijing, China). 1,5-Diphenylcarzazide was from J&K Chemical Co., LTD (Beijing, China). All solutions were prepared with deionized water with 18 MΩ cm resistivity (Millipore, Bedford, MA, USA). The stock solution of Cr(VI) and each anion and cation was prepared by dissolving the corresponding salts in deionized water.

Preparation of Fe-Gallic Acid Hybrid. We synthesized Fe-GA hybrids under solvothermal synthesis conditions by using DMF as solvent. Briefly, 4 mmol of $FeCl_2 \cdot 4H_2O$ was dissolved in 10 mL of ethanol, and then mixed with 80 mL of DMF; after that 8 mmol of gallic acid were added to the mixture under stirring. The reaction solution was transferred in a Teflon-lined stainless-steel autoclave, sealed to heat at 393 K for 24 h. The synthesized Fe-GA hybrids were black in color. The products were washed with DMF and ethanol several times and dried at 333 K under vacuum environment for 4h.

Batch Experiments. All batch experiments were conducted in 100 mL PET bottles containing 50 mL working solution with desired Cr(VI) concentration contacted with 1 g L^{-1} of Fe-GA (D). The batch reactors were placed on a KS4000 ic control (IKA, Germany) at 300 r/min at room temperature. The effect of initial Cr(VI) concentration was tested by altering the initial concentration to 100-2000 mg L^{-1}. The influence of solution pH was investigated by adjusting pH from 3.0 to 10.0 with dilute aqueous solution of HCl and NaOH. The reaction kinetic of Cr(VI) removal in water was studied following the above adsorption procedure at pH 4. At certain intervals of time, a 1 mL solution was collected, centrifuged, and analyzed for Cr(VI). The effects of coexisting anions (including chloride ions, nitrate, sulfate, and phosphate) and cations (Cu^{2+}, Ni^{2+}, Cd^{2+}, Zn^{2+}, Ba^{2+}, and Mn^{2+}) on the removal of Cr(VI) was investigated at pH 4 with 1 g L^{-1} of Fe-GA (D). The initial concentration of each anion and cation was 100 mg L^{-1}. After reaction, the samples were centrifuged at 10, 000 rpm and the supernatants were collected and analyzed for Cr(VI).

Langmuir and Freundlich adsorption models were applied to describe the equilibrium characteristics of adsorption of Cr on Fe-GA (D). The Langmuir model is based on the assumption that the adsorption takes place through monolayer adsorption on a homogeneous surface without transformation and interaction between the adsorbed molecules. The Freundlich equation is an empirical model assuming that the adsorption occurs on a heterogeneous surface or surfaces supporting sites of varied affinities. The linear form of the Langmuir isotherm equation is
expressed as:

$$\frac{c_e}{q_e} = \frac{1}{Q_{mK_L}} + \frac{C_e}{Q_m}$$

where Ce is the equilibrium concentration (mg L^{-1}), qe is the amount of adsorbate per unit mass of adsorbent at equilibrium (mg g^{-1}), Qm is the maximal adsorption

capacity (mg g^{-1}) and K_L is a constant related to the free energy of the adsorption (L mg^{-1}).
The well-known logarithmic form of the Freundlich isotherm is given as:

$$lnq_e = lnK_F + \frac{1}{n}lnC_e$$

where K_F ((mg g^{-1})(L $mg^{-1})^{1/n}$) and n are the Freundlich constants that point to the sorption capacity and adsorption intensity of the adsorbent, respectively.

The pseudo-second-order kinetic model can be expressed in the following form:

$$\frac{t}{q_t} = \frac{1}{kq_e{}^2} + \frac{t}{q_e}$$

where qe (mg g^{-1}) and qt (mg g^{-1}) are the amounts of Cr(VI) adsorbed at equilibrium and any time t (h), respectively, k is the rate constant of pseudo-second-order sorption (g mg^{-1} h^{-1}).

To test the feasibility of Fe-GA (D) for Cr(VI) removal from environmental water, batch experiments were also conducted for river water, tap water, influent and effluent of sewage treatment plant without adjusting solution pHs.

Analytical Methods. The concentration of Cr(VI) anion was determined with colorimetric method using an ultraviolet spectrophotometer at 540 nm in the presence of 1,5-diphenylcarbazide. The detection limit of the colorimetric method was 0.01 mg L^{-1} (as Cr). The concentration of total Cr after reaction, including both Cr(VI) and the produced Cr(III) species, the leached Fe cations from Fe-GA (D) in the reaction process, and the concentration of coexisting cations were measured by ICP-MS (7500A, Agilent).

Characterization of the Materials. The size and morphology of the synthesized material was surveyed using a Hitachi S-5500 field-emission scanning electron microscope (FE-SEM, Tokyo, Japan) and a JEOL JEM-2010 high-resolution transmission electron microscope (HRTEM, Kyoto, Japan). X-Ray powder diffraction (XRD, Almelo, Netherlands) which using a Cu Ka radiation ranging from 5° to 90° with a resolution of 0.02^o was utilized to analysis the crystalline. Fourier Transform infrared spectroscopy (FTIR) spectra were obtained from 4000 to 400 cm^{-1} by a NEXUS 670 Infrared Fourier Transform Spectrometer (Nicolet Thermo, Waltham, MA). The sample powder was prepared by mixing with KBr and then pressing the mixture into transparent disks. Surface area, pore size and volume were measured by Brunauer-Emmett-Teller (BET) methods (ASAP2000 V3.01A; Micromeritics, Norcross, GA). X-Ray photoelectron spectroscopy (XPS) was measured with an ESCA-Lab-200i-XL spectrometer (Thermo Scientific, Waltham, MA) with monochromatic Al Kα radiation (1486.6 eV). Zeta potential of adsorbents at different pHs were measured using Zetasizer Nano series (Malvern, United Kingdom).

Before the measurement of surface areas of the material, the as-prepared Fe-GA(D) hybrids were washed with DMF three times and then soaked with ethanol at 60^oC for three days (change fresh ethanol each day) to exchange DMF solvent in the crystal lattice of Fe-GA nanorods. After that, the Fe-GA(D) was heated at 80^oC for 4h under vacuum.

Electroplate liquids samples. Two kinds of electroplate liquids after usage were sampled directly from electroplating bath in a small zinc-plating plant in Hebei Province. The electroplate liquids contain 10% of HCl and high concentration of Fe atoms (about 2300 mg L^{-1}). The initial concentration of Cr(VI) was 20542.4 and 22638.6 mg L^{-1} respectively. We first adjusted the solution pH to about 5.0 using NaOH. And the concentration of Cr(VI) decreased to 172122.2 and 18305.5 mg L^{-1} respectively.

Table S1. Freundlich and Langmuir adsorption isotherms parameters for Cr(VI) and total Cr sorption on Fe-GA (D)

	Freundlich			Langmuir		
	K_F (mg/g) (L/mg)$^{1/n}$	$1/n$	R^2	Q_m (mg/g)	K_L (L/mg)	R^2
Cr(VI)	665.35	0.137	0.968	1709.2	0.079	0.920
Total Cr	115.55	0.433	0.994	1666.7	0.014	0.911

Table S2 Comparison of maximum adsorption capacity and optimal solution pH of Cr(VI) on Fe-GA (D) with other adsorbents

Adsorbents	Adsorption capacity (mg/g)[a]	Optimal solution pH	Temperature (°C)	Ref.
Salvinia auriculata biomass	62.2-72	2	20-30	1
Magnetic chitosan−Fe (III) hydrogel	153.8	3		2
Micro/nanoparticles of chitosan (MCH)	135.2	2		3
Spent tea and coffee dusts	44.9 and 39.0	4		4
Sulfuric acid-modified Avocado seed	333.33, 370.37, and 400	2	25, 35, and 45	5
ZVI-immobilized calcium alginate beads	320.66	7		6
Biofilm-coated nZVI−calcium alginate beads	473.9	7		6
Titanium cross-linked chitosan	171	5	25	7
Microsheets of ZnAl-LDH hexagonal nanoplates	172-223	5-6	25-45	8
Lactate-intercalated [MgAl-NO_3]-LDH	125.97	6		9
Alumium magnesium	112	4	40	10
Nanoalumina	73.2 and 59.4	7	27	11
Silane modified halloysite	37.25	3-5		12
Polyaniline/Mg/Al layered double hydroxides	393.7	2.5-5.4		13
Humic acid coated on magnetite	3.37	4-10		14
Urchin-like rutile TiO2–C nanocomposite	225	3-6		15
Amino groups modified graphene oxide	215.2	2	55	16
mesoporous carbon	165.3	3		17

microspheres				
Carbon beads	23.2-56.2	2-3		18
Cellulose derived magnetic mesoporous carbon	327.5	1.0		19
Polyethyleneimine and graphene oxide composite	581	2		20
Magnetic carbon obtained at 800°C	278.8	2		21
Activated carbon coated with quarternized poly(4-vinylpyridine)	53.7 (pH2.25) 30.7 (pH3.65) 18.9 (pH6.04)			22
Cr(VI) ion imprinted polymer	338.73	2		23
Polypyrrole-polyaniline nanofibers	227.2-294.1		25-45	24
Poly(ethylene-co-vinyl alcohol) functional nanofiber membranes	90.74-100.3	2	25-45	25
Cr(VI)-imprinted polymer	286.56	1.5-2.5		26
Poly(amidoamine)-grafted cellulose nanofibril aerogels	377.36	2		27
Crosslinked chitosan–diethylenetriaminepentaacetic acid	192.3	3		28
Polyethyleneimine functionalized eggshell membrane	169	3	35	29
MOFs based on isonicotinate N-oxide	145	2−9	25	30
Core-shell Fe3O4@MIL-100(Fe)	18	2		31
Silver-triazolate MOFs	37	5	30	32
MOFs, FIR-53 and (FIR-54)	74.2 and 103			33
Fe-GA (D)	1709.2	3-9	room temperature	This study

[a] The maximum adsorption capacity for Cr(VI) in most studies is obtained according to Langmuir adsorption model.

References

1. N. Módenes, A. P. de Oliveira, F. R. Espinoza-Quiñones, D. E. G. Trigueros, A. D. Kroumov and R. Bergamasco, Chemosphere, 2017, 172, 373.
2. Z. H. Yu, X. D. Zhang and Y. M. Huang, Ind. Eng. Chem. Res., 2013, 52, 11956.
3. J.B. Dima, C. Sequeiros and N.E. Zaritzky, Chemosphere, 2015, 141, 100.
4. K. Prabhakaran, K. Vijayaraghavan and R. Balasubramanian, Ind. Eng. Chem. Res., 2009, 48, 2113.

5. M. Bhaumik, H. J. Choi, M. P. Seopela, R. I. McCrindle and A. Maity, Ind. Eng. Chem. Res., 2014, 53, 1214.
6. K. V. G. Ravikumar, D. Kumar, G. Kumar, P. Mrudula, C. Natarajan and A. Mukherjee, Ind. Eng. Chem. Res., 2016, 55, 5973.
7. L. L. Li, H. M. Duan, X. J. Wang and C. N. Luo, New J. Chem., 2014, 38, 6008.
8. N. Kumar, L. Reddy, V. Parashar and J. C. Ngila, J. Environ. Chem. Eng., 2017, 5(2), 1718.
9. Zhang, L. Y. Luan, R. T. Gao, F. Li, Y. J. Li and T. Wu, Colloids Surf. A: Physicochem. Eng. Asp., 2017, 520, 399.
10. Y. Li, B. Gao, T. Wu, D. Sun, X. Li, B. Wang and F. Lu, Water Res., 2009, 43, 3067.
11. M. L. Paul, J. Samuel, S. B. Das, S. Swaroop, N. Chandrasekaran and A. Mukherjee, Ind. Eng. Chem. Res., 2012, 51, 15242.
12. P. Luo, J. S. Zhang, B. Zhang, J. H. Wang, Y. F. Zhao, and J. D. Liu, Ind. Eng. Chem. Res., 2011, 50, 10246.
13. K. R. Zhu, Y. Gao, X. L. Tan and C. L. Chen, ACS Sustainable Chem. Eng., 2016, 4, 4361.
14. W. J. Jiang, Q. Cai, W. Xu, M. W. Yang, Y. Cai, D. D. Dionysiou and K. E. O'Shea, Environ. Sci. Technol., 2014, 48, 8078.
15. G. D. Zou, J. X. Guo, Q. M. Peng, A. G. Zhou, Q. R. Zhang and B. Z. Liu, J. Mater. Chem. A, 2016, 4, 489.
16. He, Z. Q. Yang, J. Ding, Y. C. Chen, X. W. Tong and Y. Li, Colloids Surf. A: Physicochem. Eng. Asp., 2017, 520, 448.
17. J. G. Zhou, Y. F. Wang, J. T. Wang, W. M. Qiao, D. H. Long and L. C. Ling, J. Colloid Interface Sci., 2016, 462, 200.
18. W. Zheng, Q. D. An, Z. M. Lei, Z. Y. Xiao, S. R. Zhai and Q. M Liu, RSC Adv., 2016, 6, 104897.
19. B. Qiu, H. B. Gu, X. R. Yan, J. Guo, Y. R. Wang, D. Z. Sun, Q. Wang, M. Khan, X. Zhang, B. L. Weeks, D. P. Young, Z. H. Guo and S. Y. Wei, J. Mater. Chem. A, 2014, 2, 17454.
20. J. H. Chen, H. T. Xing, H. X. Guo, W. Weng, S. R. Hu, S. X Li, Y. H. Huang, X. Sun and Z. B. Su, J. Mater. Chem. A, 2014, 2, 12561.
21. B. Qiu, Y. R. Wang, D. Z. Sun, Q. Wang, X. Zhang, B. L. Weeks, R. O'Connor, X. H. Huang, S. Y. Wei and Z. H. Guo, J. Mater. Chem. A, 2015, 3, 9817.
22. J. Fang, Z. Gu, D. Gang, C. Liu, E. S. Ilton and B. Deng, Environ. Sci. Technol. 2007, 41, 4748.
23. Z. Q. Ren, D. L. Kong, K. Y. Wang and W. D. Zhang, J. Mater. Chem. A, 2014, 2, 17952.
24. M. Bhaumik, A. Maity, V. V. Srinivasu and M. S. Onyango, Chem. Eng. J., 2012, 181−182, 323.
25. D. Xu, K. Y. Zhu, X. T. Zheng, and R. Xiao, Ind. Eng. Chem. Res., 2015, 54, 6836.
26. L. Kong, F. Zhang, K. Y. Wang, Z. Q. Ren, and W. D. Zhang, Ind. Eng. Chem. Res. 2014, 53, 4434.
27. J. Q. Zhao, X. F. Zhang, X. He, M. J. Xiao, W. Zhang and C. H. Lu, J. Mater. Chem. A, 2015, 3, 14703.
28. R. Bhatt, B. Sreedhar and P. Padmaja, Int. J. Biol. Macromol., 2015, 74, 458.
29. B. Liu and Y. M. Huang, J. Mater. Chem., 2011, 21, 17413.
30. L. Aboutorabi, A. Morsali, E. Tahmasebi and O. Büyükgüngor, Inorg. Chem., 2016, 55, 5507.
31. Q. X. Yang, Q. Q. Zhao, S. S. Ren, Q. Q. Lu, X. M. Guo and Z. J. Chen, J. Solid State Chem.,

2016, 244, 25.
32. L. L. Li, X. Q. Feng, R. P. Han, S. Q. Zang and G. Yang, J. Hazard. Mater., 2017, 321, 622.
33. H. R. Fu, Z. X. Xu, and J. Zhang, Chem. Mater., 2015, 27, 205.

Table S3 Pseudo-second-order rate constants for the adsorption of total Cr on Fe-GA (G)

	$q_{e,\ cal}$ (mg/g)	k (g/mg h)	R^2
Total Cr	94.14	0.019	0.999

Table S4. The composition of elements on the surface of Fe-GA (D) before and after the treatment of Cr(VI)

	Fe-GA (D)	Fe-GA (D) Cr(VI) pH4	Fe-GA (D) Cr(VI) pH8
C1s	58.23	41.19	40.8
O1s	35.16	46.51	45.94
Fe2p	6.61	8.34	9.44
Cr2p		3.95	3.82

Table S5. Removal efficiency of Cr(VI) from two electroplate liquid samples

Adsorbents	Dosage of adsorbent (g L^{-1})	Removal efficiency of Cr(VI) (%)	
		sample-1	sample-2
Fe-GA(D)	2	15.9	10.7
	3	21.8	17.1
	5	35.6	24.2
	10	52.6	46.0
AC	10	19.0	17.3
Fe-GA(D)	10g/L three times	90.5	85.2
AC	10g/L three times	29.3	27.6

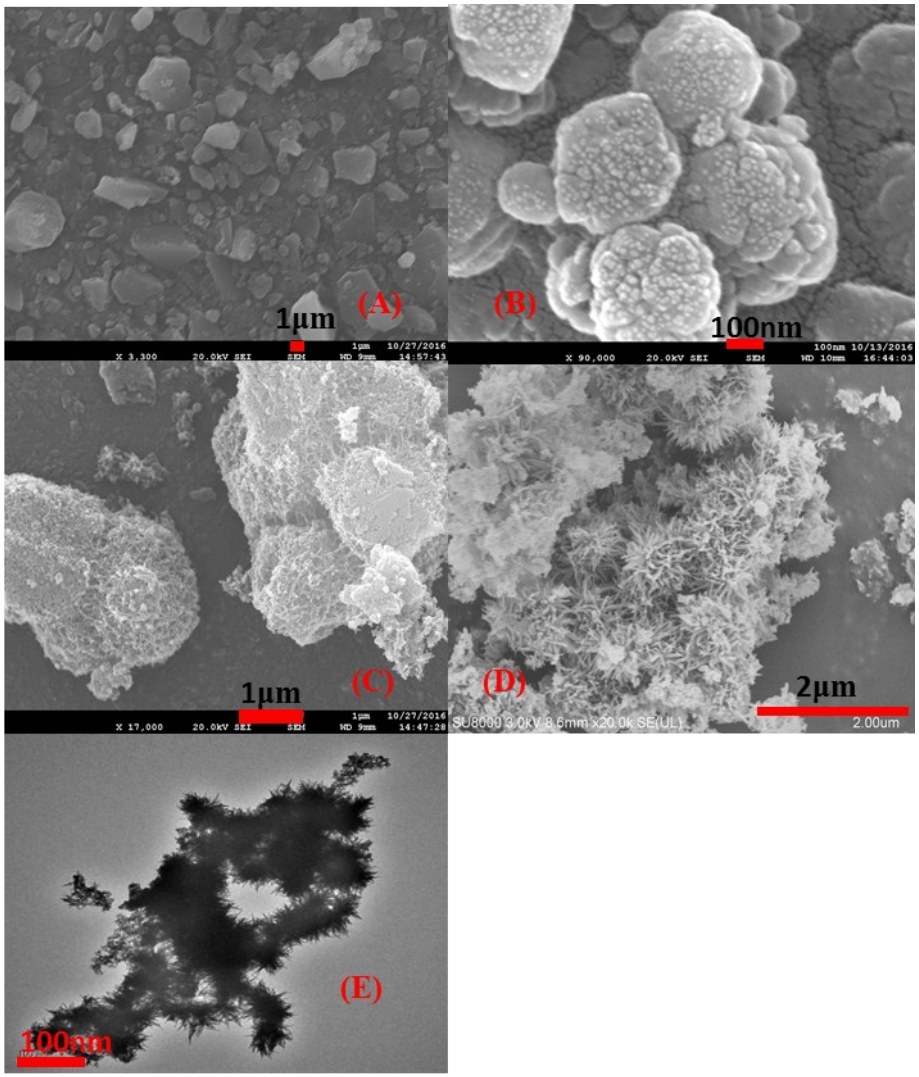

Fig. S1. The SEM images of Fe-GA (D) prepared at different reaction temperature in DMF solvent (A) 80°C, (B) 100°C, (C) 120°C, (D) 150°C, and TEM image (E) of Fe-GA hybrids obtained at 150°C.

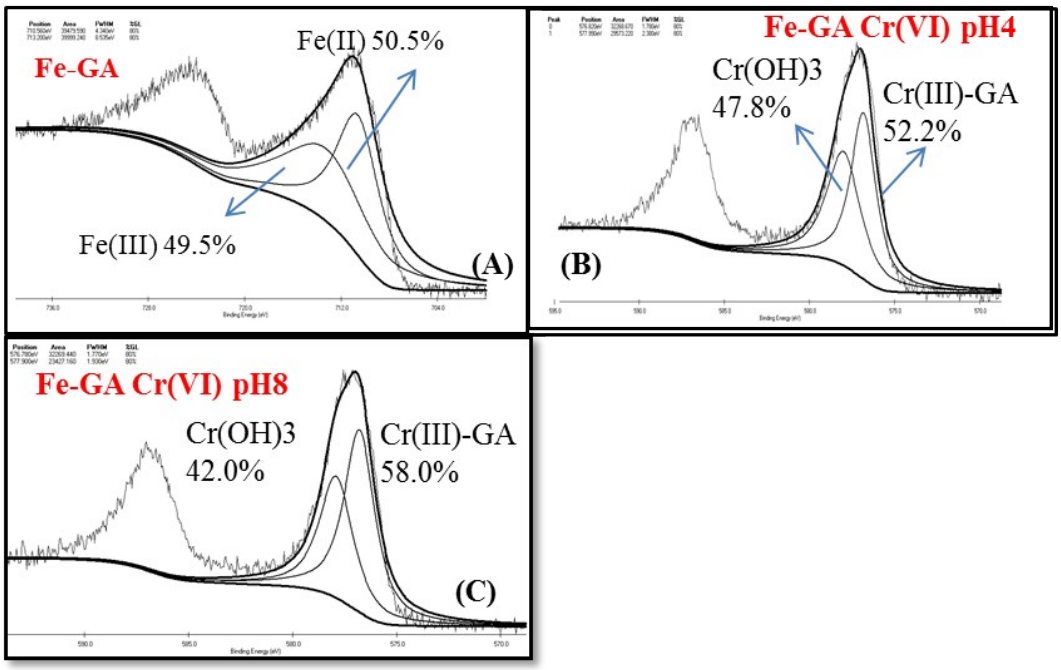

Fig. S2. Peak fitting of Fe2p spectra of Fe-GA (D) hybrids (A) and Cr 2p spectra of Fe-GA after treated with Cr(VI) at pH 4 (B), and pH 8 (C).

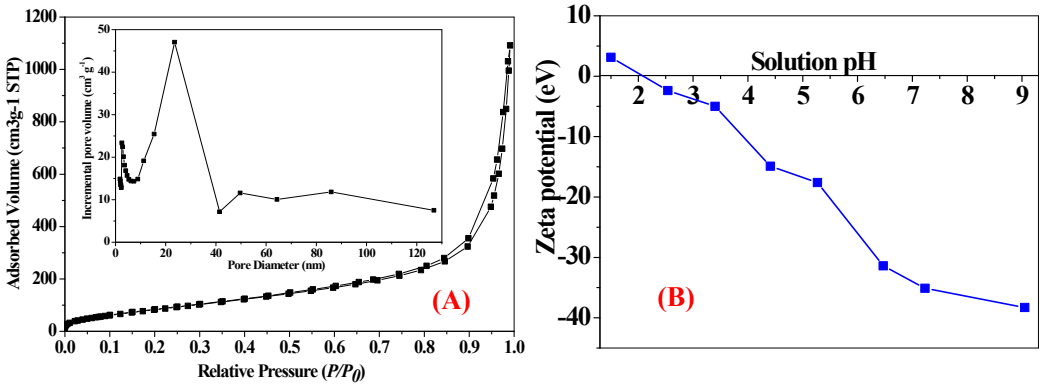

Fig. S3. N_2 adsorption–desorption isotherms of Fe-GA (D), the inset shows the distribution of pore diameter (A), and Zeta potential of Fe-GA (D) in 0.01 M $NaNO_3$ solution at different solution pHs (B). In the N_2 adsorption/desorption isotherm, a hysteresis loop at P/P_0=0.8-1.0 was observed, suggesting the surface coverage of macropores which might be the slits between Fe-GA nanorods.

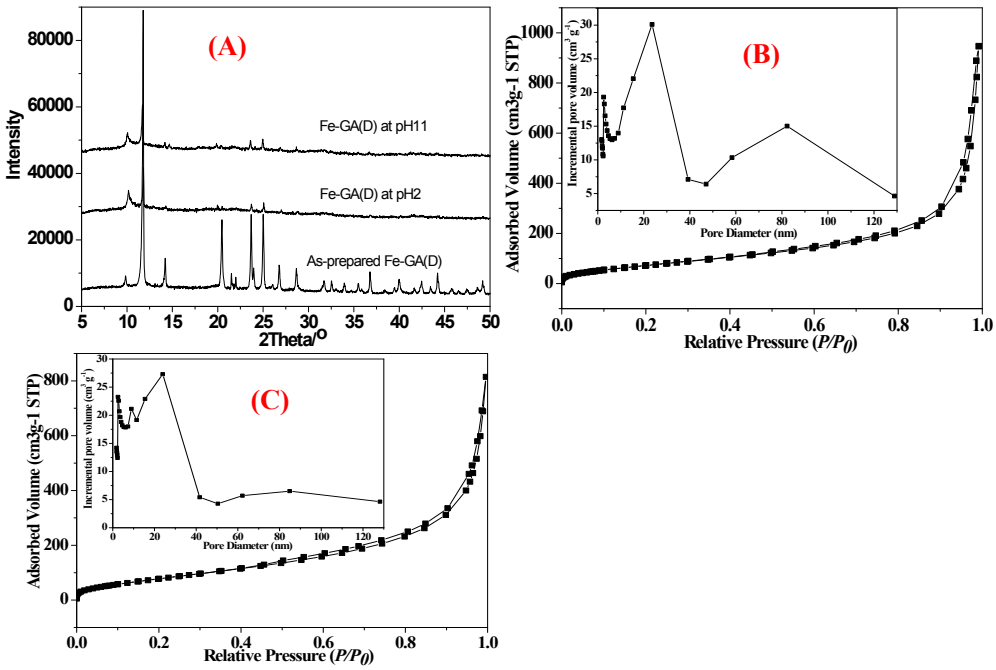

Fig. S4. XRD patterns of the as-prepared Fe-GA(D) and Fe-GA(D) treated with acid (pH=2) and alkaline (pH11) solution (A), N_2 adsorption–desorption isotherms of Fe-GA (D) treated with acid (B) and alkaline (C) solution. The insets in (B) and (C) show the distribution of pore diameter. The surface areas decreased a little, which was 257.5 and 278.7 m^2 g^{-1} as Fe-GA(D) was treated at acid (pH2) and alkaline (pH11) solution, respectively.

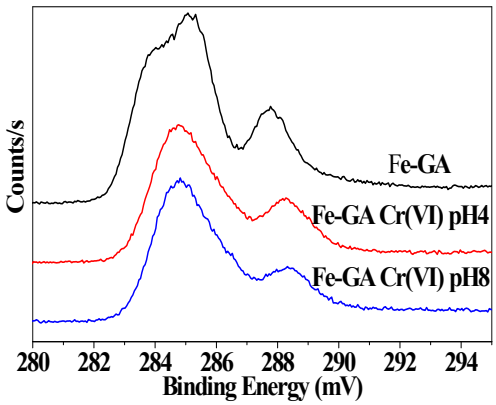

Fig. S5. C1s XPS spectra of Fe-GA (D) before and after interaction with Cr(VI)

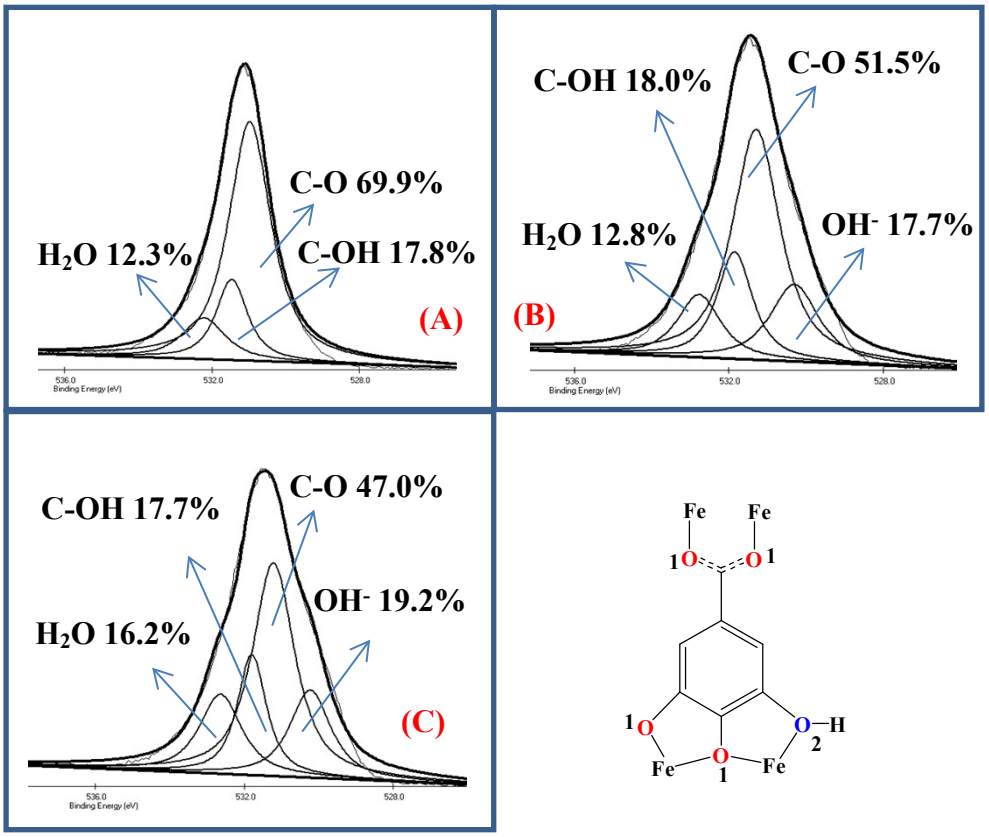

Fig. S6. Peak fitting of O1s spectra of Fe-GA (D) (A), after treated with Cr(VI) at pH 4 (B), and pH8 (C).

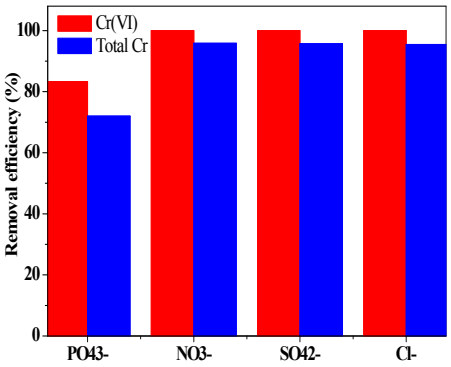

Fig. S7. Effect of coexisting anions on the removal of Cr(VI)/Cr(III) by Fe-GA (D) hybrids.

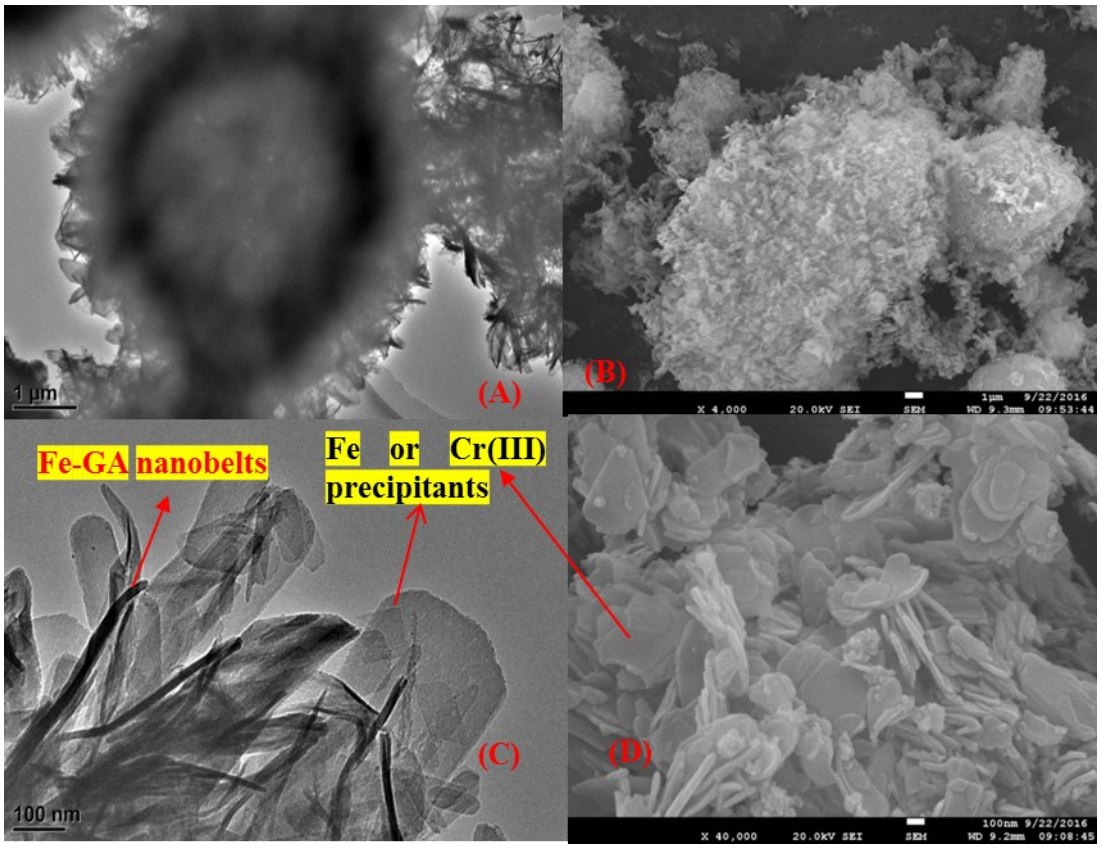

Fig. S8. FTIR spectra of Fe-GA (D) before and after interaction with Cr(VI) and Cr(III) (A), TEM (B), SEM image (C), high resolution of TEM image (E), and SEM image (E) of Fe-GA (D) after interaction with Cr(VI).

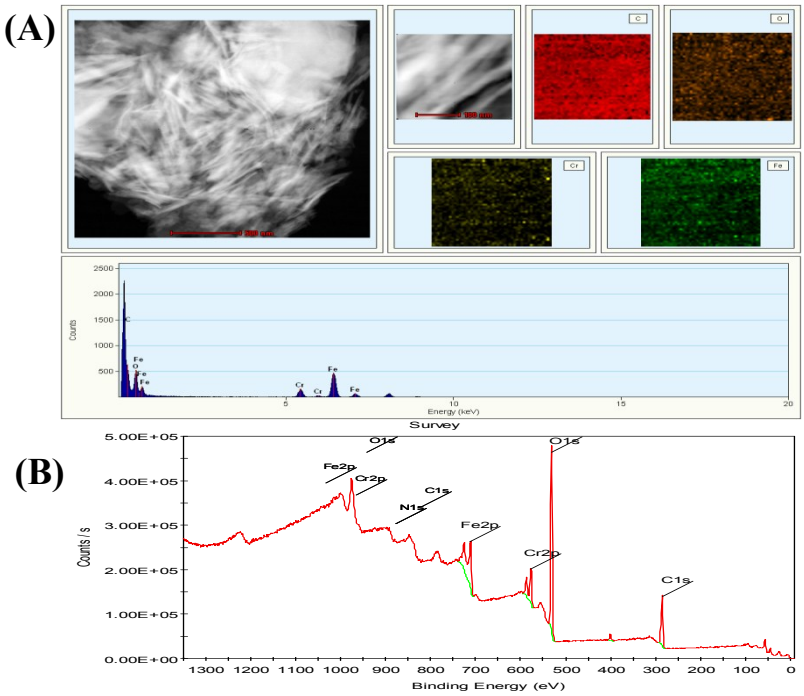

Fig. S9. STEM image and EDX mapping (A) and XPS spectra (B) of Fe-GA (D) hybrids after treatment of Cr(VI).